Wear 267 (2009) 944–953

Contents lists available at ScienceDirect

Wear

journal homepage: www.elsevier.com/locate/wear

HVOF-sprayed WC–CoCr coatings on Al alloy: Effect of the coating thickness on the tribological properties

G. Bolelli [a], L. Lusvarghi [a], M. Barletta [b,*]

[a] Department of Materials and Environmental Engineering, University of Modena and Reggio Emilia, Via Vignolese 905, I-41100 Modena (MO), Italy
[b] Department of Mechanical Engineering, University of Roma "Tor Vergata", Via del Politecnico 1, I-00133 Roma, Italy

ARTICLE INFO

Article history:
Received 27 August 2008
Received in revised form 8 December 2008
Accepted 8 December 2008

Keywords:
High Velocity Oxygen-Fuel (HVOF) spraying
Aluminium alloy
Ball-on-disk test
Cyclic impact test
Focused Ion Beam (FIB)
Vickers microhardness

ABSTRACT

The microstructure, the micromechanical properties, the wear behaviour and the impact resistance of WC–CoCr cermet coatings, deposited onto an aluminium alloy substrate by High Velocity Oxygen-Fuel (HVOF) flame-spraying, were examined as a function of the coating thickness, which was varied between 50 μm and 150 μm by performing different numbers of scans of the HVOF torch in front of the substrate. The coatings became denser and significantly harder as the number of torch scans increased: the analysis of single WC–CoCr splats by combined SEM and Focused Ion Beam (FIB) techniques enabled the interpretation of the mechanisms underlying this phenomenon. In accordance to such densification, the sliding wear resistance increased with the number of torch scans, as abrasive grooving and brittle failure mechanisms were progressively suppressed. The resistance to cyclic impact was also enhanced. In comparison to anodised films, the WC–CoCr coatings appeared much more resistant against wear and cyclic impact; specifically, three torch scans seem enough to produce a coating having suitable characteristics.

1. Introduction

Light alloys (like Al alloys) are increasingly being used for various industrial applications. Their high strength-to-density ratio and elastic modulus-to-density ratio are exploited in the production of stiff and lightweight automotive and aeronautic components [1]. They are also being proposed for plastic injection moulds, thanks to their low density (lower weight of the mould) and high thermal conductivity (more uniform temperature distribution on the mould surfaces) [2,3]. The main drawback of Al alloys is their poor tribological behaviour [2–5]: Al alloy components having to withstand contact conditions must necessarily be coated or surface-treated. Consequently, protective coatings on Al alloys are a subject of considerable technological interest.

Of the various surface treatments available for aluminium alloys, the most common ones are certainly the anodisation treatments, by which 10–50-μm thick Al_2O_3-based films (containing some hydroxides as well) are grown on a component's surface [6,7]. Anodised films are generally produced in a sulphuric or chromic acid bath at about 50 °C: above a very thin barrier layer, a thicker layer containing numerous, small columnar pores is formed; these pores are usually sealed in order to confer protectiveness against corrosive agents. Alternatively, hard anodising treatments, performed at low-temperature (≤5 °C) in sulphuric acid-based baths under high current density, produce a very hard and dense layer (free of columnar pores), which needs no sealing and provides optimized protection against wear [6,7].

Anodised films offer interesting characteristics; however, they also imply some drawbacks. The intrinsic brittleness of these purely ceramic films may induce cracking and delamination from the substrate under severe operating conditions. The processing time needed to produce quite thick anodised films (≥50 μm) can be quite long (some hours), especially in the case of the low-temperature hard anodising process [6]. Anodisation also requires careful surface pre-treatment steps, including cleaning, etching and polishing, which increase processing cost and time. The outcome of the anodisation treatment is also dependent on the alloy composition [6–8]; specifically, some alloys yield anodised films having poor characteristics.

Therefore, other coating technologies could be preferable in some applications. Specifically, thermal spraying techniques already enjoy a significant industrial diffusion in order to coat steels and other metal substrates, thanks to their ability to produce high-performance layers. With reference to the above-mentioned drawbacks of anodisation treatments, thermal spraying techniques are definitely less sensitive to the nature of the substrate, they do not require complex surface pre-treatments (generally, surface preparation for thermal spraying only involves de-greasing and grit-blasting), they enable the deposition of quite thick layers (≥100 μm) with satisfactory productivity, and are also very flexible concerning the choice of the coating material [9–11]. Materials providing the proper compromise between hardness and tough-

* Corresponding author. Tel.: +39 06 72597168; fax: +39 06 2021351.
E-mail address: Massimiliano.barletta@uniroma2.it (M. Barletta).

0043-1648/$ – see front matter © 2009 Elsevier B.V. All rights reserved.
doi:10.1016/j.wear.2008.12.066

ness can therefore be selected [11,12]. Particularly, HVOF-sprayed WC-based cermets (e.g. WC–Co, WC–CoCr) have been shown to possess excellent tribological properties [13–16]; indeed, they combine very high hardness with satisfactory toughness [11,17], as Co-based metal matrixes possesses ductility and excellent wettability toward the carbide grains.

Accordingly, WC-based coatings on steel substrates have already been technically validated as an alternative to hard chrome plating, particularly for the most severe operating conditions [13,14,16,18]. The nature of the substrate (for instance, steel vs. aluminium), generally speaking, can affect the outcome of every coating process, but, in the case of thermal spraying techniques, this influence is not too large, so that it may be reasonably conjectured that HVOF-sprayed WC-based coatings can also offer good tribological properties when deposited onto Al substrates [2], even though some differences, in comparison to the traditional steel substrates, are likely to exist. Research studies concerning WC-based HVOF-sprayed coatings on light alloys (Al alloys or Mg alloys) are therefore being carried out [2–4,19–22], but they are still not very numerous. One very important aspect, which has not been explicitly considered yet in the above-mentioned studies, is the effect of the coating thickness on its properties, in particular on the tribological performance: this issue is particularly critical when dealing with soft substrates, as Al alloys are. Generally speaking, if a coating is very thin, a significant share of the stress distribution produced by the contact with a rigid counterbody has to be born by the substrate [23,24]: in these conditions, light alloys could deform plastically due to their high ductility. If the coating is much harder and less ductile, premature failure of the coating itself or of the coating–substrate interface becomes possible. On the other hand, however, the production of a thinner coating is clearly more economical: as the torch has to perform fewer scans in front of the substrate, the processing time is decreased, and lower amounts of gas and powder are consumed. The best compromise should therefore be sought for.

The aim of this research was therefore to assess the effect of the thickness on the micromechanical properties and the tribological behaviour of WC–CoCr coatings deposited on an Al alloy substrate by HVOF-spraying using different numbers of torch scans (from 2 to 5). The effect of adding a thin HVOF-sprayed Ni-based bond coat (single torch scan, in order not to increase the overall processing time excessively) was also considered in this paper. The performances of the WC–CoCr coatings were compared to those of two kinds of anodised films: a protective anodised film, produced by the ordinary process in a sulphuric acid-based bath and sealed in a Ni^{2+}, F^--containing aqueous solution, and a hard-anodised film, produced by the low-temperature treatment.

2. Experimental

WC–10%Co–4%Cr coatings were produced by depositing a commercially available spray powder (Praxair 1350VM, agglomerated and sintered, −45 + 15 μm nominal particle size distribution) onto aluminium alloy 6082-T6 plates of (80 mm × 80 mm × 8 mm) size, using the Praxair-Tafa JP5000 HVOF torch, operated with the parameters listed in Table 1. The plates were previously grit-blasted to $R_a \approx 6$ μm using a manual vacuum-operated Norblast blasting machine, with 500 μm angular alumina grits (Metcolite-C, Sulzer Metco). Coatings with increasingly large thickness were produced by performing a total of 2, 3, 4 and 5 complete torch scans in front of the substrate, respectively. On half of the plates, a Ni bond coat (powder: Praxair 1166F, −53 + 20 μm nominal particle size distribution) was HVOF-deposited in a single torch scan, using deposition parameters also listed in Table 1.

Single WC–CoCr splats were also collected onto ground aluminium and carbon steel plates, using the same deposition parameters as in Table 1 but with much greater traverse speed.

Table 1
HVOF-deposition parameters.

	WC–10%Co–4%Cr	Ni
Barrel length (mm)	152.4	101.6
O_2 flux (Sm^3/s)	1.456×10^{-2}	1.416×10^{-2}
Kerosene flux (Sm^3/s)	6.3×10^{-6}	5.3×10^{-6}
Carrier gas flux (Sm^3/s)	1.8×10^{-4}	1.7×10^{-4}
Feeder plate speed (1/s)	5.5	4.5
Stand-off distance (mm)	380	355
Combustion chamber pressure (bar)	6.76	6.27
Torch traverse speed (mm/s)	500	500
Interpass spacing (mm)	3	3
Substrate temperature (°C)	<150	<150

For comparative purpose, part of the plates were polished to $R_a \approx 0.02$ μm and anodised using two different processes, representative of the industrial state-of-the-art in anodisation treatments: a conventional process, performed at 50 °C in a sulphuric acid-based bath and followed by a sealing treatment in a Ni^{2+}, F^--containing aqueous solution, and a hard anodisation process performed at 2 °C in a sulphuric acid-based bath. Both processes were carried out in an industrial plant using proprietary parameters; the thickness of the resulting films was close to 50 μm.

The phase composition of the HVOF-sprayed WC–CoCr coatings was characterised by X-ray diffraction (XRD), using Cu $K\alpha_1$ radiation (X'Pert Pro, PANAlytical, Eindhoven, The Netherlands), and their microstructure was observed by scanning electron microscopy (SEM, XL30 and Quanta-200, FEI, Eindhoven, The Netherlands) on cross-sections, prepared by cold-mounting in resin, grinding using SiC papers (up to 2500 mesh) and polishing using diamond slurries (up to 0.5 μm).

The Vickers microhardness (Micro-Combi Tester, CSM Instruments, Peseux, Switzerland) of the WC–CoCr coatings was measured on the polished cross-sections using an indentation load of 1 N (20 indentations per sample, performed in the middle of the coating thickness). Unidirectional dry sliding tribological tests were performed in ball-on-disk configuration, using a pin-on-disk tribometer (High-Temperature Pin-on-Disk Tribometer, CSM Instruments) equipped with sintered WC–6%Co spherical pins, 3 mm diameter. Test conditions included 10 N normal load, 0.20 m/s relative sliding speed, 5000 m overall sliding distance, 5 mm wear track radius; tests were run at (21 ± 2) °C temperature and (56 ± 2)% relative humidity. These very severe contact conditions (the maximum hertzian contact pressure which would be produced on a flat steel sample would be of about 2600 MPa) were chosen after some preliminary tests, in order to be able to produce a detectable wear scar on the cermet-coated samples. The WC–CoCr coatings were manually polished to $R_a \approx 0.02$ μm using diamond papers (very smooth surface finishes are typically required for thermally sprayed WC–CoCr coatings intended for sliding wear applications, an example being provided in ref. [16]) and ultrasonically degreased in acetone before tribological testing. The wear rate of the samples was measured by optical confocal profilometry (Conscan Profilometer, CSM Instruments); the friction coefficient was monitored during the test by a load cell. The wear scar morphology was studied by SEM. The same tribological test was also performed on the anodised films, for reference.

Cyclic impact tests were performed on WC–CoCr coatings and on anodised films: a quenched and tempered C100KU steel ball (39 mm diameter), connected to an overall weight of 12 N, was cyclically raised and released from a height of 90 mm (impact energy 1.08 J), dropping onto the sample surface (45 impacts/min). The total number of impacts was set at 1000. Under these impact conditions, the resulting contact stress distribution significantly

affects the substrate and causes visible plastic deformation of the coated system, so that the ability of the coating to conform to the substrate deformation and to resist cracking and spallation phenomena is effectively probed. The surfaces and polished cross-sections of the samples were inspected by SEM and by optical microscopy.

In order to get a better insight into the deposition mechanisms of HVOF-sprayed WC–CoCr coatings onto an Al alloy substrate in comparison to those on a steel substrate, the single splats collected on ground Al and steel surfaces were observed by SEM and sectioned *in situ* by Focused Ion Beam (FIB) technique, using a dual beam machine (StrataTM DB235, FEI) combining a high-resolution FIB column equipped with a Ga Liquid Metal Ion Source (LMIS) and a SEM column equipped with Schottky Field Emission Gun (SFEG) electron source. The section was produced using an ion beam current of 7 nA and subsequently polished using an ion beam current of 300 pA.

3. Results

3.1. Microstructural and micromechanical characterization

The XRD patterns of all HVOF-sprayed coatings exhibit no perceivable differences in the type and amount of phases, regardless of the thickness and of the presence or absence of the Ni bond coat (Fig. 1). Moreover, peaks relating to Al and/or to Ni could not be detected in any case, probably due to the low penetration depth of the X-rays into the cermet coating.

SEM micrographs indicate that the WC–CoCr coatings do not display a very large porosity (Fig. 2). Their porosity, however, seems to be affected by the number of torch scans; indeed, image analysis indicates that the porosity values decrease as the number of torch scans increases (Table 2). Specifically, the most remarkable variations occur from 2 to 3 scans and from 3 to 4 scans, whereas the thickest coatings (4 and 5 scans) display quite similar porosity. The Ni bond coat deposited by a single torch scan appears very thin and inhomogeneous (Fig. 3); its presence does not affect the previously noted relation between porosity and number of torch scans (Table 2).

All of the as-deposited coatings have an average roughness $R_a \approx 3.6\,\mu m$.

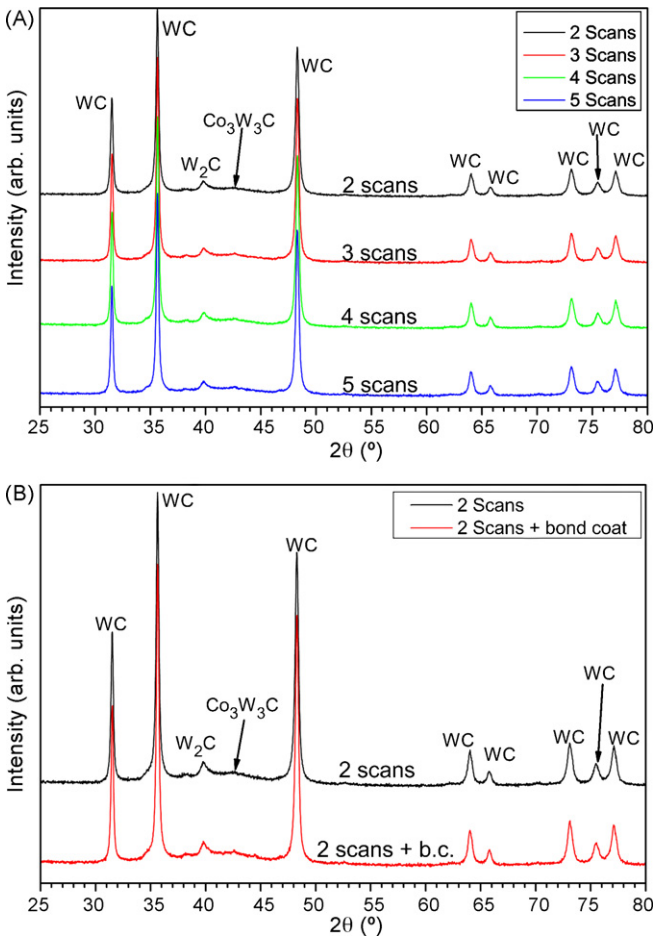

Fig. 1. Comparison between the XRD patterns of WC–CoCr coatings having different thickness (a) and deposited with or without Ni bond coat (b).

In order to obtain additional information on the deposition mechanisms of WC–CoCr particles onto different substrates, the SEM + FIB analysis of single splats deposited on Al substrates was conducted. Upon impact, the HVOF-sprayed WC–CoCr parti-

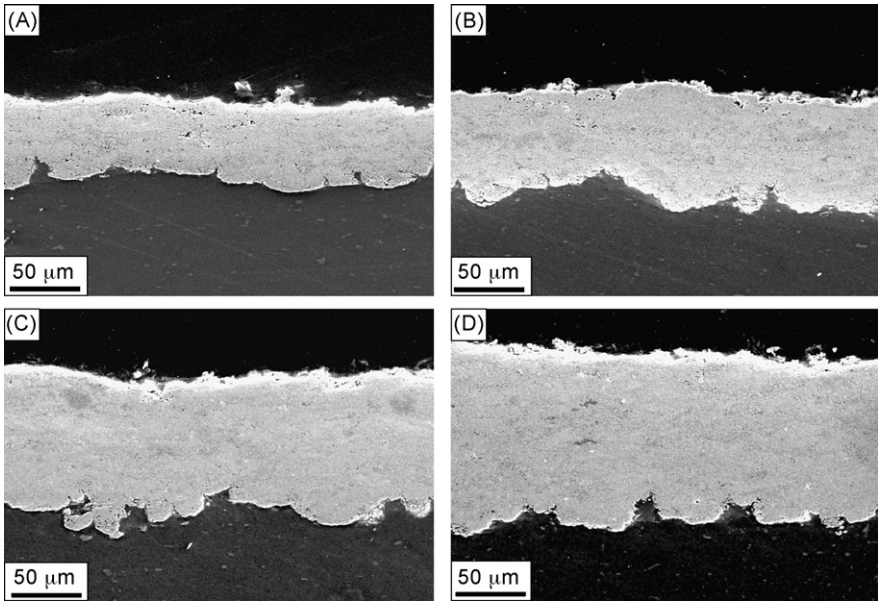

Fig. 2. SEM micrographs of the cross-sections of the WC–CoCr coatings, HVOF-sprayed onto Al substrates using 2 (a), 3 (b), 4 (c) and 5 (d) torch scans.

Table 2
Thickness and porosity of the HVOF-sprayed WC–CoCr coatings, as determined by image analysis.

Coating	Porosity (%)	Thickness (μm)
2 scans	3.2 ± 1.1	58.6 ± 9.6
3 scans	1.5 ± 0.8	79.2 ± 10.2
4 scans	0.8 ± 0.2	104.4 ± 12.0
5 scans	0.5 ± 0.2	136.8 ± 10.9
2 scans + bond coat	2.7 ± 1.1	47.5 ± 9.4
3 scans + bond coat	2.6 ± 0.9	74.2 ± 8.0
4 scans + bond coat	0.7 ± 0.2	104.3 ± 11.6
5 scans + bond coat	0.4 ± 0.2	124.7 ± 11.7

cles deform the soft aluminium substrate remarkably, penetrating deeply into its surface (Fig. 4a). The cermet particles, therefore, cannot spread and flatten extensively, so that small defects and pores remain inside the non-flattened particle, as highlighted by FIB sections (Fig. 4b, see circle).

By contrast, single splats collected on steel clearly show that particles sprayed on a harder surface spread extensively, with minimal substrate deformation (Fig. 4c and d), and do not retain as many defects as the particles directly deposited onto the soft Al surface. It is noted that similar, well-flattened splats are also recognizable on top of the thicker WC–CoCr coatings (Fig. 5, the circle indicates a clearly recognizable flattened splat).

The Vickers microhardness of the coating increases with the number of scans (Fig. 6). Specifically, the largest increase in hardness occurs from 2 to 3 torch scans, whereas, at higher number of scans, the increase is less remarkable. The hardness of the 2-scan coating is significantly lower than the values reported in the pertinent literature for analogous HVOF-sprayed WC–CoCr coatings [13,25], whereas the hardness of the coatings with 3 or more scans approaches or overcomes 1100$HV_{0.1}$, which is comparable to good-quality cermet coatings [13,25]. The presence or absence of the Ni bond coat (samples with bond coat are identified by the label "bc") does not affect the hardness of WC–CoCr layers significantly, except, maybe, for the 2-scan coating.

3.2. Sliding wear resistance

The wear rates measured after the ball-on-disk tests match the Vickers microhardness results (Fig. 7): the wear rate decreases as the coating thickness increases, the largest difference being the one between 2 torch scans and 3 torch scans. Moreover, the 2 scan-coating shows slightly lower wear rate when deposited on the Ni bond coat (label "bc" in Fig. 7), consistently with its slightly higher hardness.

SEM micrographs show some abrasive grooving (Fig. 8a) and limited brittle fracture phenomena (Fig. 8a—circled area, Fig. 8b—detail) in the 2-scan WC–CoCr coating, which features lower hardness and higher defectiveness. By contrast, thicker coatings do not exhibit perceivable grooving or fracture (Fig. 8c): wear loss seems only due to the removal of the metal matrix between the carbide grains (Fig. 8d), the typical wear mechanism of bulk (sintered) cermets and of those HVOF-sprayed cermets where alteration of the metal matrix has been kept to moderate levels during deposition [26]. The wear rate of the hard anodised film, by contrast, is higher by three orders of magnitude; the conventional, sealed anodised film was completely removed well before the end of the 5000-m long test. Delamination of the cermet coating from the substrate was never observed, even for the thinnest layers.

3.3. Cyclic impact tests

After the cyclic impact test, none of the HVOF-coated samples exhibits any apparent crack or defect along the coating–substrate interface (Fig. 9a and b). Moreover, the WC–CoCr coatings deposited with higher numbers of torch scans (≥3) do not undergo a large overall impact damage: their two main degradation mechanisms seem to be transverse cracking (Fig. 9a, arrow) and localised near-surface delamination (Fig. 9a, circle), but the occurrence of both phenomena is very limited (as shown by Fig. 9a itself). Accordingly, in these coatings, no circumferential cracking occurs along the periphery of the impact region (Fig. 9c) and only a very limited amount of cracks can be recognised in the middle of that region (Fig. 9d, label 1), together with some transfer material coming from the steel ball (Fig. 9d, label 2).

The 2-scan coating also displays almost no transverse cracking, but it suffers extensive near-surface damage, leading to the removal of non-negligible amounts of material by delamination (Fig. 9b).

In comparison to the WC–CoCr layers (especially to those deposited with more than 2 torch scans), the anodised films were much more severely cracked: they showed evidence of delamination inside the impact area (overview in Fig. 10a, detail in Fig. 10b)

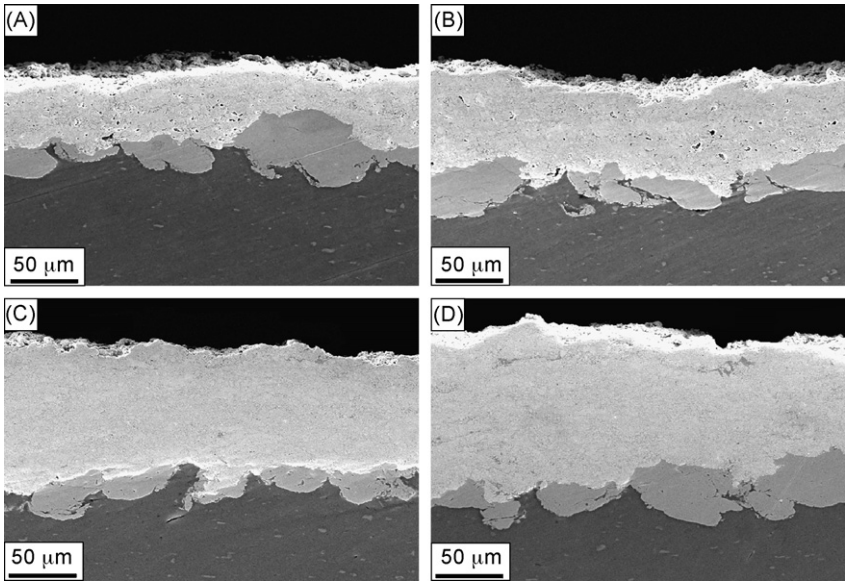

Fig. 3. SEM micrographs of the cross-sections of the WC–CoCr coatings, HVOF-sprayed onto Al substrates with Ni bond coat. Cermet layers were deposited using 2 (a), 3 (b), 4 (c) and 5 (d) torch scans.

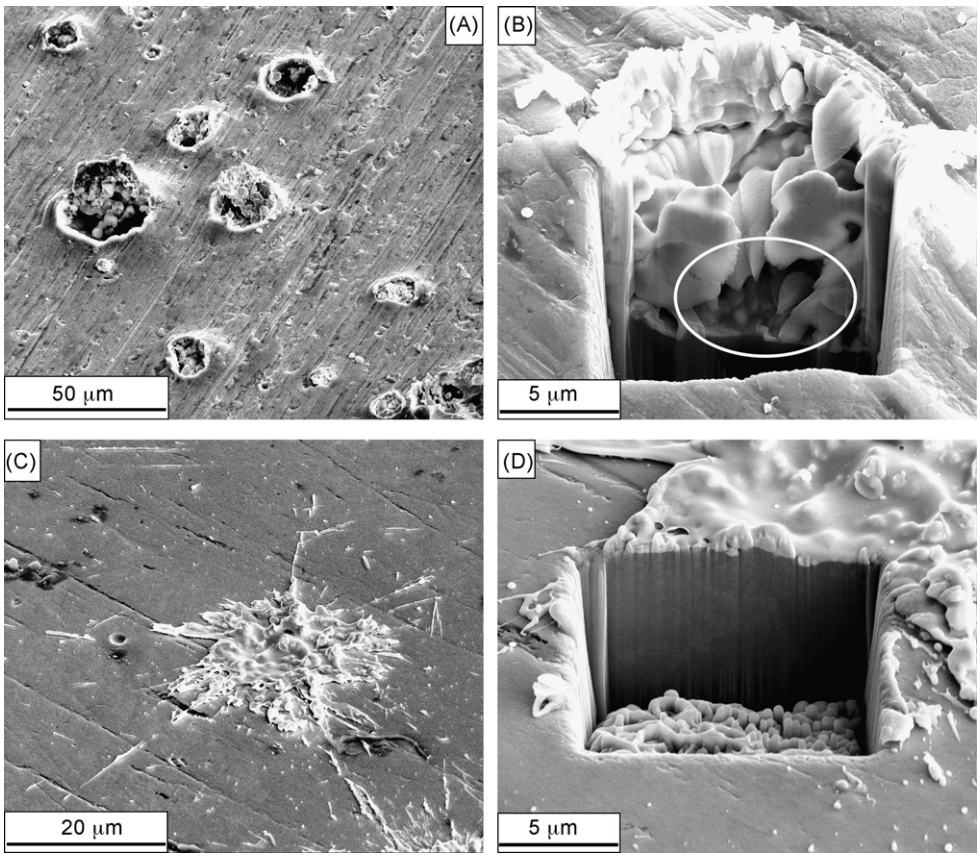

Fig. 4. SEM micrographs of single WC–CoCr splats on Al and steel surfaces: (a) splats on Al surface; (b) FIB section of a splat on Al surface, highlighting small defects (circle); (c) splat on steel surface; (d) FIB section of the splat on steel surface.

and also displayed many radial cracks extending out of the impact area (Fig. 10c).

4. Discussion

Decarburization and carbide dissolution have been kept to a very moderate level during the HVOF-deposition of the present WC–CoCr coatings; indeed, the diffraction peaks of W_2C and Co_3W_3C have very low intensity (Fig. 1). As suggested in [27], an approximate "index of carbide retention" (Eq. (1)) can be defined as

$$I = \frac{I_{WC}}{I_{WC} + I_{W_2C}} \quad (1)$$

where: I_{WC} = intensity of the (1 0 0) peak of WC at $2\theta = 35.6^\circ$; I_{W_2C} = intensity of the (1 0 1) peak of W_2C at $2\theta = 39.6^\circ$.

All of the coatings have almost identical I values of (0.91 ± 0.01), thus confirming the high level of WC retention; indeed, in ref.

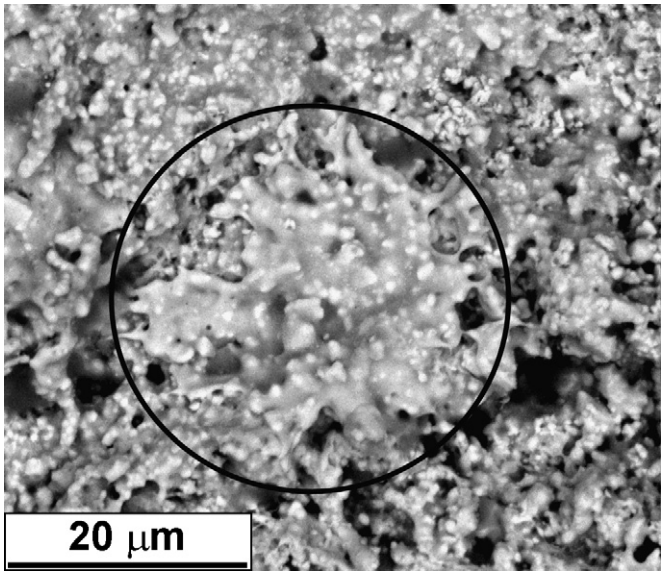

Fig. 5. SEM micrograph of the top surface of the HVOF-sprayed WC–CoCr coating (5 scans, no bond coat).

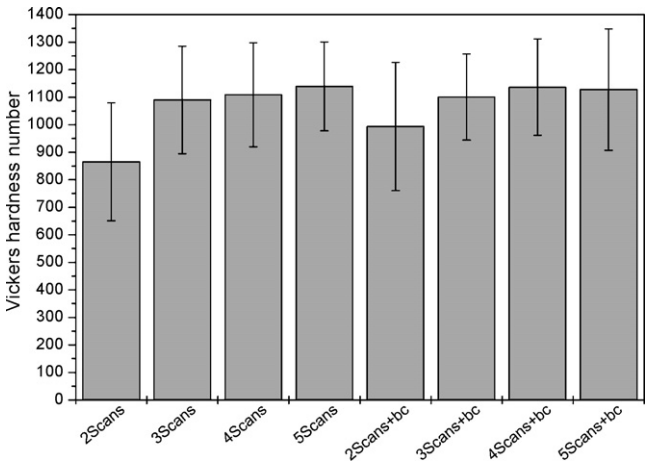

Fig. 6. Vickers microhardness of WC–CoCr layers, measured in the middle of the coating thickness. *Note*: bc = sample with Ni bond coat.

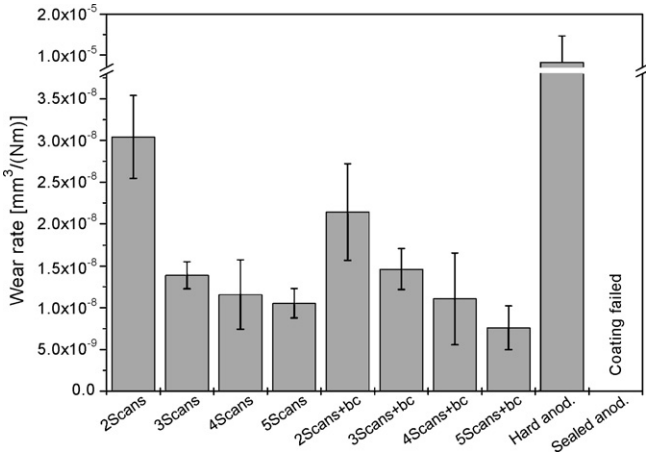

Fig. 7. Wear rates measured after ball-on-disk dry sliding tests. Note that the sealed anodised layer was completely removed after less than 1000 m, exposing the substrate to severe wear. *Note*: bc = sample with Ni bond coat.

[27], typical values of I for HVOF-sprayed WC-based coatings are declared to be around 0.85. Retention of WC is generally desirable, in order to optimise the tribological performance of the coating. When WC decomposes or dissolves into the matrix, indeed, two unfavourable phenomena simultaneously occur: the hard phase (conferring wear resistance) is lost and the ductile metal matrix (providing toughness) is embrittled [28–30]. On the other hand, however, no WC decomposition may indicate insufficient particle heating, resulting in defective coatings having poor interlamellar cohesion [26]. In the present case, the low porosity, high hardness and excellent wear and impact resistance of the coatings deposited with three or more torch scans clearly indicate that a good compromise between retention of the carbide phase and sufficient heating of the powder particles was achieved during spraying.

Nonetheless, the above-mentioned properties vary quite considerably with the number of torch scans; in particular, the largest differences exist between coatings deposited with fewer scans. The microstructural analysis (Figs. 2 and 3 and Table 2), indeed, reveals that the coatings become denser as the number of torch scans increases, the most remarkable improvements occurring at low number of torch scans (from 2 to 3 and from 3 to 4). The densification is accompanied by a progressive strengthening of the coating material; accordingly, the Vickers microhardness increases with the number of scans (Fig. 6): the largest increase occurs from 2 to 3, whereas, at higher number of scans, the variation is less remarkable.

This peculiar phenomenon has not been observed nor discussed in the literature yet; therefore, single splats were studied by SEM and FIB in order to obtain an understanding of the deposition mechanisms of HVOF-sprayed cermet particles onto a soft aluminium alloy substrate. These particles impinge in a semi-solid condition, because most of the WC phase does not melt in the HVOF flame: this has been suggested by previous literature works [31] and it is clearly revealed, in the present case, by the low level of carbide dissolution; moreover, numerical simulations have indicated that the temperature of the cermet particles during HVOF-spraying is typically well below the melting point of the carbide phase, and that part of the metal matrix could remain below the melting point as well [32]. The high-velocity impingement of these semi-solid particles exerts a high pressure on the substrate [31]; consequently, the soft Al substrate is plastically deformed, as clearly shown in Fig. 4a and b. Analogous plastic deformation phenomena have already been described in previous observations of single splats sprayed onto soft substrates by the high-velocity oxygen-fuel or air-fuel processes [19,33]. Perhaps, a further contribution to such deformation might also come from localised melting of the substrate material at the impact location, because of the heat input coming both from the gas jet and from the molten particle [34,35], although this phenomenon is more likely to occur during plasma spraying of very high melting point material and has not yet been considered explicitly for the HVOF-spraying process.

Consequently, the particles penetrate deeply into the substrate surface, as noted in Section 3.1: they achieve an excellent bonding to the substrate, but they cannot spread, so that they retain small pores and defects. Because of this phenomenon, when spraying cermet coatings on soft substrates by the HVOF technique, the first layers can be expected to be somewhat porous. This indeed occurs in the presently considered 2-scan coating.

The decrease in porosity as the coating thickness increases can be justified by two reasons. First of all, as the torch scans again and again in front of the substrate, the impact of new WC–CoCr particles peens the previously deposited layers intensively and densifies

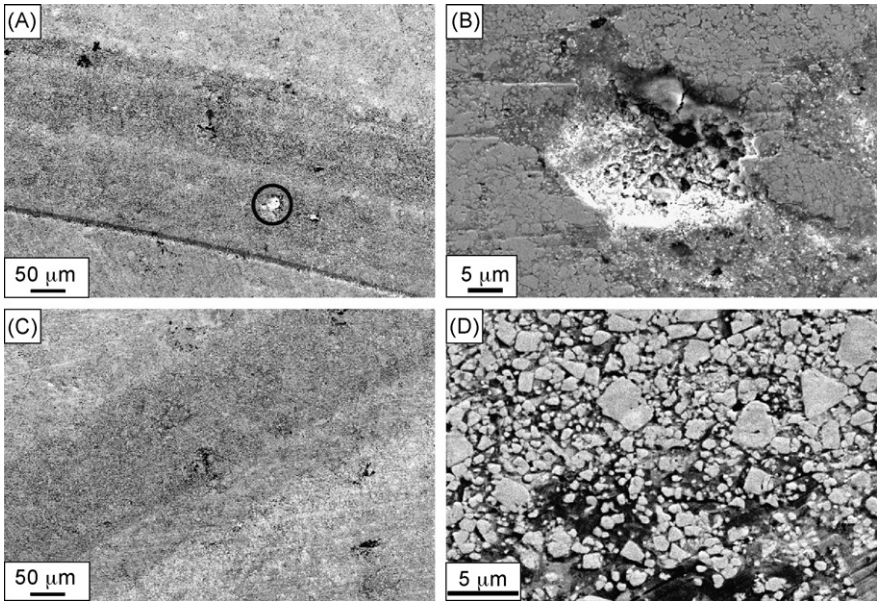

Fig. 8. SEM micrographs of the ball-on-disk wear scars on WC–CoCr coatings: (a) 2-scan coating, general view; (b) 2-scan coating, detail of area circled in panel A; (c) 4-scan coating, general view; (d) 4-scan coating, detail.

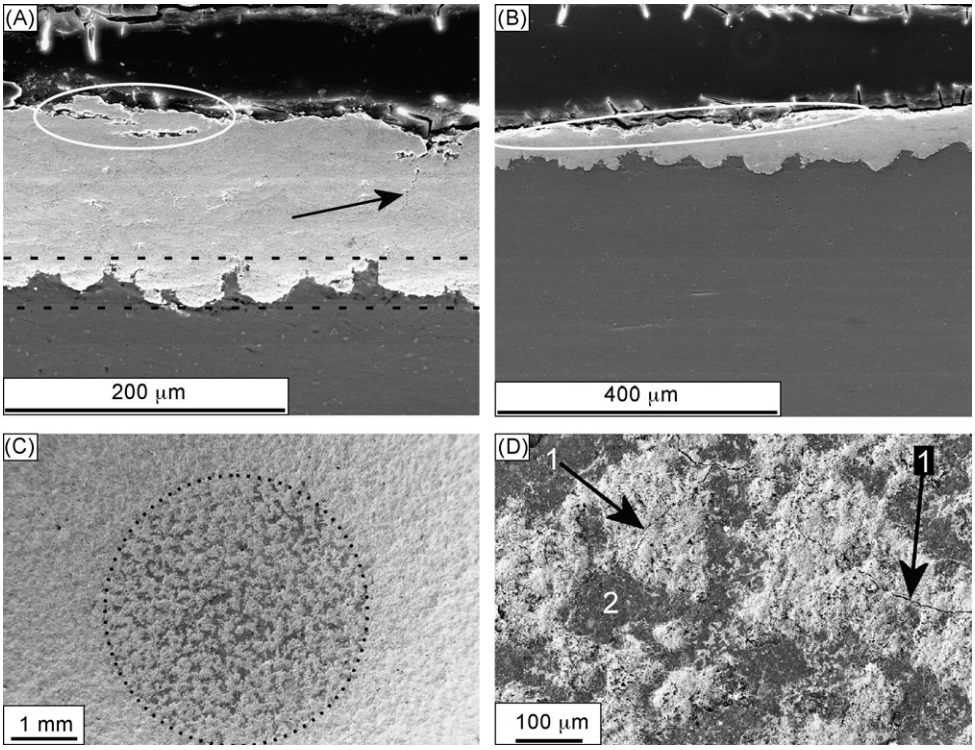

Fig. 9. SEM micrographs of the WC–CoCr layers subjected to the cyclic impact test: (a) 5-scan coating, cross-section (arrow: transverse cracking; circle: near-surface delamination; dotted lines indicate the rough coating-substrate interface); (b) 2-scan coating, cross-section (circle: near-surface delamination); (c) 3-scan cermet coating, low magnification surface view (dotted circle: impact area); (d) 3-scan cermet coating, high magnification surface view (1: transverse cracks, 2: transferred steel).

them very effectively, because of the above-mentioned high impact pressures [31]. In the pertinent literature, the occurrence of peening actions during HVOF-spraying has already been described, and it has been shown to produce significant effects on characteristics like porosity and residual stresses [26,36,37]. This process explains why the underlying layers become denser as the coating thickness increases; however, Figs. 2 and 3 clearly indicate that even the topmost layers of the thicker coatings are very dense, even though they have not undergone any peening action. Consequently, a second phenomenon should be taken into account: whereas the deposition of the first coating layers is affected by the low hardness of the Al substrate (as described above), the newly incoming particles encounter a much harder surface, once a sufficiently large number of torch scans has been performed. Their deposition and flattening mechanisms are therefore modified. WC–CoCr particles sprayed onto the harder steel surface, indeed, flatten extensively and do not retain any defect (Fig. 4c and d). Similar, well-flattened splats are also seen on top of the thicker WC–CoCr coatings (Fig. 5). The porosity of the cermet coatings therefore decreases not only because the underlying coating layers are peened and densified by the deposition of a new layer, but also because the new layer is probably less defective than the first layers.

Clearly, the effects of both phenomena (the peening action and the flattening mechanism modification) are most remarkable at low number of torch scans; when several scans have already been performed, instead, the underlying layers have already undergone much peening and the flattening mechanism has already changed, so that further improvement in density and strength are scarce.

The increase in hardness is definitely consistent with this interpretation. When the number of scans is low (2 scans), the material located in the middle of the coating has not been intensively peened yet, and it comes from layers containing intrinsic defects, as explained previously. By contrast, after several scans, the material in the middle of the coating has undergone more peening cycles and also comes from layers which are intrinsically less defective, because particles deposited onto previous WC–CoCr layers do not retain defects.

The presence or absence of the Ni bond coat does not affect the porosity or the hardness of the WC–CoCr layers significantly, except (possibly) for the hardness of the 2-scan coating. This may be due to the fact that the Ni bond coat, in spite of its large inhomogeneity (it almost looks like individual splats, rather than a real homogeneous layer), provides a slightly harder underlayer, enabling better spreading of the cermet splats; consequently, the 2-scan coating on the Ni bond coat is somewhat harder than the one directly deposited onto the Al substrate. Consistently, the former is also slightly thinner than the latter (Table 2): presumably, the harder Ni bond coat favours the rebounding of a larger fraction of the semi-solid WC–CoCr particles, slightly impairing the deposition efficiency.

These densification and strengthening phenomena are of significant importance, as they have a direct, non-negligible influence on the wear resistance of the coating. The 2-scan coating (which has not been intensively peened yet), indeed, suffers both grooving and brittle fracture wear. Brittle fracture is probably due to the presence of weak points in this layer, which has not been densified by intensive peening yet. Near-surface cracks propagate from these points and detach some material. Grooving is probably produced by debris particles being trapped between the sample and the counterbody: because of the low hardness of the 2-scan coating, these particles may plastically deform it. Both phenomena are progressively suppressed by the densification and strengthening achieved with increasing number of torch passes, so that a remarkable improvement is achieved when passing from 2 to 3 scans and minor improvements are achieved when performing further scans (Fig. 7). It is important to remark that, under the present ball-on-disk test conditions, most of the hertzian contact stress distribution is concentrated on the coating rather than on the substrate or on

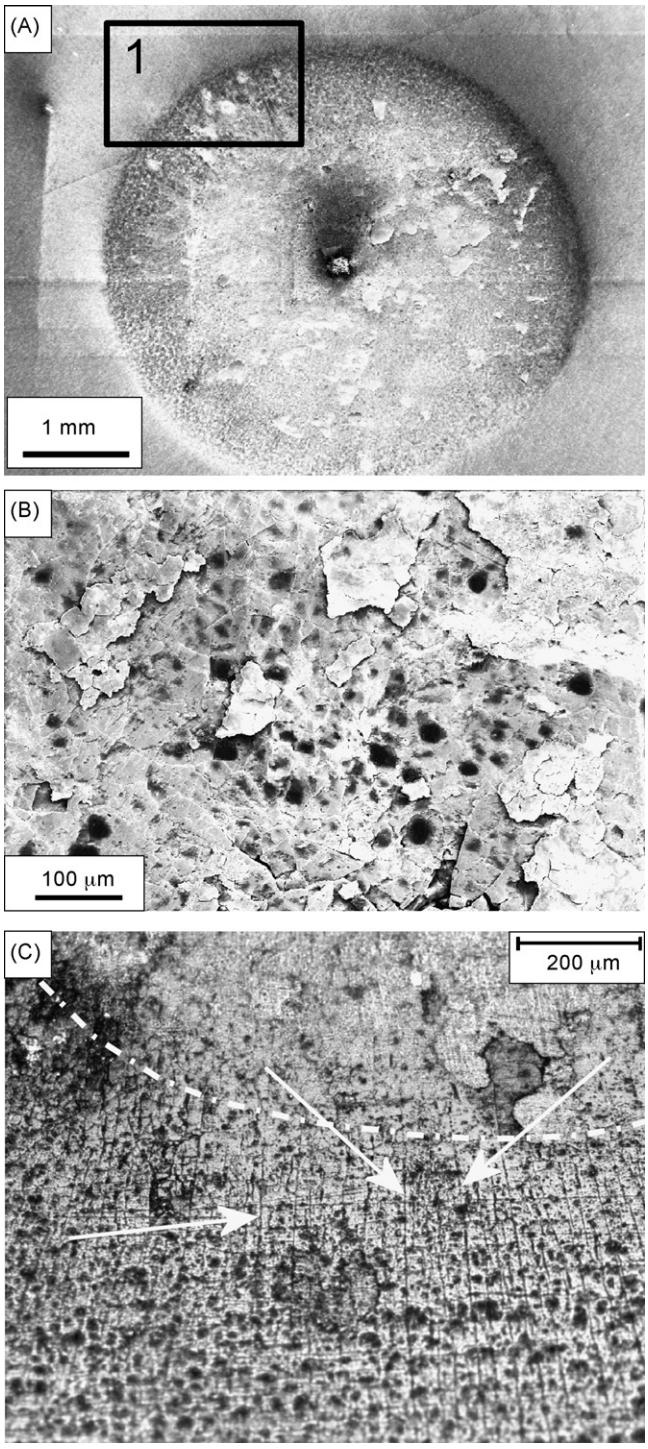

Fig. 10. Surface of the hard anodised layer after cyclic impact testing: (a) SEM micrograph, low magnification view; (b) SEM micrograph, high magnification view of region 1 in panel (a); (c) optical micrograph, high magnification view of region 2 in panel (a) (dash-dot line: limit of the impact area; arrows: radial cracks propagating out of the impact area).

the interface, even for the thinnest 2-scan layer. Indeed, an approximate estimation, which can be obtained by applying the Hertz's relations to a sphere-on-flat contact where the elastic properties of the flat are those of the WC–CoCr layer ($E \approx 260$ GPa [38], $\nu \approx 0.28$ [39]), indicates that the maximum sub-surface shear stress of about 895 MPa is located at a depth of about 19 μm. This test, therefore, is capable of selectively probing the effects of the intrinsic properties of the coating (its cohesion and strength) on the wear resistance; consequently, the densification effect, rather than the increase in thickness, is dictating the previously noted improvements.

Moreover, the 2-scan coating shows slightly lower wear rate when deposited on the Ni bond coat, consistently with its slightly higher hardness. This result corroborates to the previous hypothesis of a somewhat better spreading of WC–CoCr particles on the Ni bond coat.

In any case, the wear rates shown in Fig. 7 are definitely low: specifically, the wear rates of the coatings deposited with 3 or more torch scans are around or below 1×10^{-8} mm^3/(Nm). This value can certainly be regarded as representative of a very mild wear regime, if compared to literature data concerning cermet coatings (for instance, refs. [26,40,41]) or bulk ceramics; specifically, for the latter materials, mild wear is considered to take place at wear rates below 10^{-6} mm^3/(Nm) [42]. The wear rate of the hard anodized film, by contrast, is higher by three orders of magnitude; the conventional, sealed anodized film was completely removed well before the end of the 5000-m long test. As previously discussed, the chosen set of spray parameters provided a good compromise between carbide retention and particle heating, capable of optimising the tribological performance of the coating [43].

The strength of the interfacial bonding between the coating and the substrate and the overall mechanical behaviour of the coating + substrate system, which were not probed by the ball-on-disk test, are instead of the utmost importance in determining the results of cyclic impact test, which heavily affects the substrate, because of the large ball diameter and the impact energy. The present results reveal a good interfacial strength under localized contact conditions, as the interface between the cermet layers and the aluminium substrate is free of defects (Fig. 9a and b). The excellent interlocking achieved by the cermet particles penetrating deeply into the aluminium substrate (as shown by the FIB analysis, Fig. 4b) is the most likely reason for the excellent interfacial bonding. Moreover, the studies dealing with the behaviour of hard films on ductile substrates, mentioned in the introduction [23,24], generally assume a sharp, planar interface between the two elements; in the present case, however, the interface between the WC–CoCr coating and the aluminium substrate is extremely rough (Fig. 9a, see dotted lines). The penetration of the cermet particles into the aluminium surface (which has also been roughened by grit-blasting before the deposition of the coatings), indeed, creates a sort of "graded" intermediate region between the pure WC–CoCr coating and the pure aluminium substrate, a few tens of microns thick (Fig. 9a, dotted lines). This sort of "graded" region prevents the abrupt transition in mechanical properties which would occur along a perfectly smooth interface. The importance of accounting for the existence of such "graded" region at the interface between a thermally sprayed coating and a very rough substrate surface has already been pointed out in studies dealing with thermal barrier coatings [44].

The damage found in the cermet coatings after cyclic impact is due to two different mechanisms, as introduced in Section 3.3: transverse cracking and near-surface delamination. The latter phenomenon is probably related to the severe localised stress concentrations which may arise at some asperities of the rough as-deposited surface. If defects are present in those locations, cracks can form and propagate in the near-surface region. Accordingly, the delamination is more extensive in the defective 2-scan layer, where weak interlamellar boundaries and pores are more numerous. This mechanism is probably similar to the one leading to brittle fracture wear during ball-on-disk sliding tests. The lower defectiveness of the coatings deposited with several torch scans, by contrast, reduces the possibility of delamination. Transverse cracks arise from a different process. Theoretical analyses and experimental observations predict the formation of transverse cracks in hard and brittle layers deposited onto soft substrates during severe localised contacts. Specifically, circumferential cracks are predicted to develop along

the periphery of the impacted region and radial cracks in its middle [45]. The extent of such cracking in all of the present WC–CoCr coatings, however, is very limited; therefore, these layers would seem to behave in a ductile manner, conforming quite well to the substrate's deformation. The absence of a sharp interface and the presence of the above-mentioned "graded" layer may play a role in helping the coating's compliance. By contrast, in a previous literature paper [46] where single impact tests (with a wide range of impact energy values) were performed on WC–CoCr cermet coatings deposited onto a carbon steel substrate, significant circumferential cracking was noted even at the lowest impact energy condition. The presently considered WC–CoCr coatings deposited onto an aluminium alloy substrate would therefore seem to exhibit superior compliance than those deposited onto a steel substrate; indeed, although the impact energy in the present test is about half of the minimum impact energy employed in ref. [46], the present impacts are repeated 1000 times. The reasons for this significantly different behaviour may lie either in the different overall mechanical response of the WC–CoCr/steel and WC–CoCr/aluminium systems, or in the different deposition conditions employed in the present paper and in ref. [46]. More detailed investigations on this subject are outside the aim of the present paper: future work will be intended to address the differences between the impact behaviour of cermet coatings deposited onto aluminium and steel substrates.

Finally, it is very important to remark that the brittle anodized films are much less compliant than the WC–CoCr cermet layers; indeed, they undergo severe transverse cracking and extensive near-surface delamination.

5. Conclusions

WC–CoCr cermet coatings were deposited onto AA 6082T6 plates by HVOF-spraying. The thickness of the coatings was varied in the 50–150 μm range by performing a different number of torch scans in front of the substrate.

This change was found to have a major influence on the coatings' characteristics. Thinner coatings are somewhat more defective, because the flattening of cermet particles impacting onto the soft Al surface is restrained by the deformation of the surface itself, so that the particles retain small pores. Thicker coatings, deposited by performing several torch scans, are denser because of two reasons. First, as a new layer is deposited, the high velocity impact of the particles peens the previously deposited material and densifies it. Secondly, the new particles can flatten more efficiently, as they impact on a much harder surface (the previously deposited coating layers); therefore, the new coating layers are less defective than the first ones.

These microstructural changes have important consequences on all of the mechanical and functional properties of the coatings. As the number of torch scans increases, indeed, the hardness of the cermet coating improves, the sliding wear rate is significantly decreased, and less damage is found after cyclic impact testing. In particular, the largest differences exist between the properties of the coatings deposited using 2 and 3 torch scans: when the number of torch scans is low, the densification effects obtained by performing an additional scan are the most remarkable; further improvements are progressively less significant.

Although the extensive deformation of the Al substrate upon impingement of the HVOF-sprayed cermet particles is a source of defectiveness, it results in an excellent interfacial adhesion between the coating and the substrate; moreover, a sort of "graded" layer (a few tens of microns thick) between the cermet coating and the aluminium substrate is produced in this way. The cermet coatings are therefore capable of sustaining cyclic impact conditions with no interfacial cracking or delamination.

The effect of a thin Ni bond coat was also checked: except for the 2-scan cermet coating, such very thin and irregular bond coat does not produce any major improvement in the microstructural, mechanical and tribological characteristics of the cermets.

Acknowledgements

The authors are grateful to Mr. Fabio Pighetti Mantini and Ing. Andrea Bassani for their assistance with the experimental activities. The authors also acknowledge the contribution of Mr. Enrico Gualtieri and Dr. Giancarlo Gazzadi (University of Modena and Reggio Emilia, Department of Physics) for the FIB analysis. Thanks to Mr. Gadda (Mochem s.r.l., Modena, Italy) for performing the anodization treatments.

Partly supported by PRRIITT (Regione Emilia-Romagna), Net-Lab "Surface & Coatings for Advanced Mechanics and Nanomechanics" (SUP&RMAN).

References

[1] M.F. Ashby, Y.J.M. Bréchet, D. Cebon, L. Salvo, Selection strategies for materials and processes, Mater. Des. 25 (2004) 51.
[2] J.A. Picas, T.A. Forn, R. Rilla, E. Martín, HVOF thermal sprayed coatings on aluminium alloys and aluminium matrix composites, Surf. Coat. Technol. 200 (2005) 1178–1181.
[3] G.J. Gibbons, R.G. Hansell, Down-selection and optimization of thermal-sprayed coatings for aluminum mould tool protection and upgrade, J. Thermal Spray Technol. 15 (2006) 340–347.
[4] B. Wielage, A. Wank, H. Pokhmurska, T. Grund, C. Rupprecht, G. Reisel, E. Friesen, Development and trends in HVOF spraying technology, Surf. Coat. Technol. 201 (2006) 2032–2037.
[5] G.W. Stachowiak, A.W. Batchelor, Engineering Tribology Butterworth-Heinemann 483-570.
[6] H. Takahashi, Aluminum anodizing, in: Corrosion: Fundamentals, Testing, and Protection ASM Handbook, vol. 13A, ASM International, Materials Park, OH, USA, 2003, pp. 736–740.
[7] P.G. Sheasby, R. Pinner, The Surface Treatment and Finishing of Aluminum and its Alloys, ASM International, Finishing Publications Ltd., Stevenage, Materials Park, OH, USA, UK, 2001.
[8] I. Tsangaraki-Kaplanoglou, S. Theohari, T. Dimogerontakis, Y.-M. Wang, H.-H. Kuo, S. Kia, Effect of alloy types on the anodizing process of aluminum, Surf. Coat. Technol. 200 (2006) 2634–2641.
[9] D.E. Crawmer, Thermal spray processes, in: J.R. Davis (Ed.), Handbook of Thermal Spray Technology, ASM International, Materials Park, OH, USA, 2004, pp. 54–84.
[10] P. Fauchais, A. Vardelle, B. Dussoubs, Quo Vadis thermal spraying? J. Thermal Spray Technol. 10 (2001) 44–66.
[11] H. Herman, S. Sampath, R. McCune, Thermal spray: current status and future trends, in: S. Sampath, R. McCune (Eds.), Thermal-Spray Processing of Materials, MRS Bulletin—July 2000, Materials Research Society International, Warrendale, PA, USA, 2000, pp. 17–25.
[12] C.C. Berndt, in: J.R. Davis (Ed.), Material Categories for Thermal Sprayed Coatings Handbook of Thermal Spray Technology, ASM International, Materials Park, OH, USA, 2004, pp. 142–168.
[13] A. Wank, B. Wielage, H. Pokhmurska, E. Friesen, G. Reisel, Comparison of hardmetal and hard chromium coatings under different tribological conditions, Surf. Coat. Technol. 201 (2006) 1975–1980.
[14] G. Bolelli, V. Cannillo, L. Lusvarghi, S. Riccò, Mechanical and tribological properties of electrolytic hard chrome and HVOF-sprayed coatings, Surf. Coat. Technol. 200 (2006) 2995–3009.
[15] D.W. Wheeler, R.J.K. Wood, Erosion of hard surface coatings for use in offshore gate valves, Wear 258 (2005) 526–536.
[16] B. Sartwell, K. Legg, J. Sauer, Validation of WC/Co HVOF Thermal Spray Coatings as a Replacement for Hard Chrome Plating On Aircraft Landing Gear, U.S. Department of Defense Environmental Security Technology Certification Program (ESTCP) and Joint Group on Pollution Prevention (JG-PP) joint test report, prepared by U.S. Hard Chrome Alternatives Team (HCAT), 21 November 2002.
[17] M. Watanabe, A. Owada, S. Kuroda, Y. Gotoh, Effect of WC size on interface fracture toughness of WC–Co HVOF sprayed coatings, Surf. Coat. Technol. 201 (2006) 619–627.
[18] G. Bolelli, R. Giovanardi, L. Lusvarghi, T. Manfredini, Corrosion resistance of HVOF-sprayed coatings for hard chrome replacement, Corros. Sci. 48 (2006) 3375–3397.
[19] M. Parco, L. Zhao, J. Zwick, K. Bobzin, E. Lugscheider, Investigation of HVOF spraying on magnesium alloys, Surf. Coat. Technol. 201 (2006) 3269–3274.
[20] J.E. Gray, B. Luan, Protective coatings on magnesium and its alloys—a critical review, J. Alloys Compd. 336 (2002) 88–113.
[21] M. Magnani, P.H. Suegama, N. Espallargas, S. Dosta, C.S. Fugivara, J.M. Guilemany, A.V. Benedetti, Influence of HVOF parameters on the corrosion and wear

resistance of WC–Co coatings sprayed on AA7050 T7, Surf. Coat. Technol. 202 (2008) 4746–4757.
[22] C.J. Villalobos-Gutiérrez, G.E. Gedler-Chacón, J.G. La Barbera-Sosa, A. Piñeiro, M.H. Staia, J. Lesage, D. Chicot, G. Mesmacque, E.S. Puchi-Cabrera, Fatigue and corrosion fatigue behavior of an AA6063-T6 aluminum alloy coated with a WC–10Co–4Cr alloy deposited by HVOF thermal spraying, Surf. Coat. Technol. 202 (2008) 4572–4577.
[23] A.C. Fisher-Cripps, B.R. Lawn, A. Pajares, L. Wei, Stress analysis of elastic–plastic contact damage in ceramic coatings on metal substrates, J. Am. Ceram. Soc. 79 (1996) 2619–2625.
[24] K. Holmberg, A. Laukkanen, H. Ronkainen, K. Wallin, S. Varjus, J. Koskinen, Tribological contact analysis of a rigid ball sliding on a hard coated surface Part II: Material deformations, influence of coating thickness and Young's modulus, Surf. Coat. Technol. 200 (2006) 3810–3823.
[25] J. Barber, B.G. Mellor, R.J.K. Wood, The development of sub-surface damage during high energy solid particle erosion of a thermally sprayed WC–Co–Cr coating, Wear 259 (2005) 125–134.
[26] Q. Yang, T. Senda, A. Ohmori, Effect of carbide grain size on microstructure and sliding wear behaviour of HVOF-sprayed WC–12%Co coatings, Wear 254 (2003) 23–34.
[27] C. Bartuli, T. Valente, F. Cipri, E. Bemporad, M. Tului, Parametric study of an HVOF process for the deposition of nanostructured WC–Co coatings, J. Thermal Spray Technol. 14 (2005) 187–195.
[28] E. López Cantera, B.G. Mellor, Fracture toughness and crack morphologies in eroded WC–Co–Cr thermally sprayed coatings, Mater. Lett. 37 (1998) 201–210.
[29] R. Schwetzke, H. Kreye, Microstructure and properties of tungsten carbide coatings sprayed with various high velocity oxygen fuel spray systems, J. Thermal Spray Technol. 8 (1999) 433–439.
[30] D.A. Stewart, P.H. Shipway, D.G. McCartney, Abrasive wear behaviour of conventional and nanocomposite HVOF-sprayed WC–Co coatings, Wear 225–229 (1999) 789–798.
[31] Y.-Y. Wang, C.-J. Li, A. Ohmori, Examination of factors influencing the bond strength of high velocity oxy-fuel sprayed coatings, Surf. Coat. Technol. 200 (2006) 2923–2928.
[32] S. Kamnis, S. Gu, T.J. Lu, C. Chen, Computational simulation of thermally sprayed WC–Co powder, Comp. Mater. Sci. 43 (2008) 1172–1182.
[33] W. Trompetter, M. Hyland, D. McGrouther, P. Munroe, A. Markwitz, Effect of substrate hardness on splat morphology in high-velocity thermal spray coatings, J. Thermal Spray Technol. 15 (2006) 663–669.
[34] L. Li, X.Y. Wang, G. Wei, A. Vaidya, H. Zhang, S. Sampath, Substrate melting during thermal spray splat quenching, Thin Solid Films 468 (2004) 113–119.
[35] W. Zhang, G.H. Wei, H. Zhang, L.L. Zheng, D.O. Welch, S. Sampath, Toward the achievement of substrate melting and controlled solidification in thermal spraying, Plasma Chem. Plasma Process. 27 (2007) 717–736.
[36] S. Kuroda, Y. Tashiro, H. Yumoto, S. Taira, H. Fukanuma, S. Tobe, Peening action and residual stresses in high-velocity oxygen fuel thermal spraying of 316 L stainless steel, J. Thermal Spray Technol. 10 (2001) 367–374.
[37] P. Bansal, P.H. Shipway, S.B. Leen, Effect of particle impact on residual stress development in HVOF sprayed coatings, J. Thermal Spray Technol. 15 (2006) 570–575.
[38] G. Bolelli, V. Cannillo, L. Lusvarghi, T. Manfredini, Wear behaviour of thermally sprayed ceramic oxide coatings, Wear 261 (2006) 1298–1315.
[39] S.-H. Leigh, C.C. Berndt, Modelling of elastic properties of plasma sprayed deposits with ellipsoid-shaped voids, Acta Mater. 47 (1999) 1575–1586.
[40] Q. Yang, T. Senda, A. Hirose, Sliding wear behavior of WC–12% Co coatings at elevated temperatures, Surf. Coat. Technol. 200 (2006) 4208–4212.
[41] H. Du, C. Sun, W. Hua, T. Wang, J. Gong, X. Jiang, S.W. Lee, Structure, mechanical and sliding wear properties of WC–Co/MoS_2–Ni coatings by detonation gun spray, Mater. Sci. Eng. A 445–446 (2007) 122–134.
[42] K. Kato, K. Adachi, Wear of advanced ceramics, Wear 253 (2002) 1097–1104.
[43] C. Verdon, A. Karimi, J.-L. Martin, Microstructural and analytical study of thermally sprayed WC–Co coatings in connection with their wear resistance, Mater. Sci. Eng. A 234–236 (1997) 731–734.
[44] J.T. De Masi Marcin, K.D. Sheffler, S. Bose, Mechanisms of degradation and failure in a plasma-deposited thermal barrier coating, ASME J. Eng. Gas Turbine Power 112 (1990) 521–528.
[45] H. Chai, B.R. Lawn, Fracture mode transitions in brittle coatings on compliant substrates as a function of thickness, J. Mater. Res. 19 (2004) 1752–1761.
[46] C. Deng, M. Liu, C. Wu, K. Zhou, J. Song, Impingement resistance of HVAF WC-based coatings, J. Thermal Spray Technol. 16 (2007) 604–609.